Auxin triggers pectin modification during rootlet emergence in white lupin

François Jobert, Alexandre Soriano, Laurent Brottier, Célia Casset, Fanchon Divol, Josip Safran, Valérie Lefebvre, Jérôme Pelloux, Stéphanie Robert, Benjamin Péret

Pelloux Jerome (Orcid ID: 0000-0002-9371-1711)
PERET Benjamin (Orcid ID: 0000-0003-1336-0796)

Auxin triggers pectin modification during rootlet emergence in white lupin

François Jobert [1, 2], Alexandre Soriano [1], Laurent Brottier [1], Célia Casset [1], Fanchon Divol [1], Josip Safran [3], Valérie Lefebvre [3], Jérôme Pelloux [3], Stéphanie Robert [2*], Benjamin Péret [1*].

Affiliations

[1] IPSiM, Univ Montpellier, CNRS, INRAE, Supagro, 34060 Montpellier, France

[2] Umeå Plant Science Centre (UPSC), Department of Forest Genetics and Plant Physiology, Swedish University of Agricultural Sciences, 901 83 Umeå, Sweden

[3] UMR INRAE 1158 BioEcoAgro, BIOPI Biologie des Plantes et Innovation, SFR Condorcet FR CNRS 3417, Université de Picardie, 80039 Amiens, France

*For correspondence:

stephanie.robert@slu.se (+ 46 (0) 907868609); benjamin.peret@cnrs.fr (+ 33 (0) 499612859)

ORCID:

François Jobert: 0000-0002-1939-2214; Laurent Brottier: 0000-0002-8584-2199; Josip Safran: 0000-0003-0582-7528; Valérie Lefebvre: 0000-0003-4482-3810; Jérôme Pelloux: 0000-0002-9371-1711; Stéphanie Robert: 0000-0002-0013-3239; Benjamin Péret: 0000-0003-1336-0796

Preprint Server: this manuscript was deposited on BioRxiv on July 19th, 2021 under the DOI number https://doi.org/10.1101/2021.07.19.452882

Number of items: 6 Main Figures (all in colour), 10 Supplemental Figures (all in colour), 5 Supplemental Tables, Supplemental Methods.

Word count: Summary (226), Significance statement (64), Introduction (811), Methods (939), Results (3240), Discussion (1244).

This article has been accepted for publication and undergone full peer review but has not been through the copyediting, typesetting, pagination and proofreading process which may lead to differences between this version and the Version of Record. Please cite this article as doi: 10.1111/tpj.15993

Summary

Emergence of secondary roots through parental tissue is a highly controlled developmental process. Although the model plant *Arabidopsis* has been useful to uncover the predominant role of auxin in this process, its simple root structure is not representative of how emergence takes place in most plants, which display more complex root anatomy. White lupin is a legume crop producing structures called cluster roots, where closely spaced rootlets emerge synchronously. Rootlet primordia push their way through several cortical cell layers while maintaining the parent root integrity, reflecting more generally the lateral root emergence process in most multilayered species. In this study, we showed that lupin rootlet emergence is associated with an upregulation of cell wall pectin modifying and degrading genes under the active control of auxin. Among them, we identified *LaPG3*, a polygalacturonase gene typically expressed in cells surrounding the rootlet primordium and we showed that its downregulation delays emergence. Immunolabeling of pectin epitopes and their quantification uncovered a gradual pectin demethylesterification in the emergence zone, which was further enhanced by auxin treatment, revealing a direct hormonal control of cell wall properties. We also report rhamnogalacturonan-I modifications affecting cortical cells that undergo separation as a consequence of primordium outgrowth. In conclusion, we describe a model of how external tissues in front of rootlet primordia display cell wall modifications to allow for the passage of newly formed rootlets.

Keywords: Auxin, Cell wall, *Lupinus albus* (white lupin), Pectin, Root development.

Significance statement

The process of secondary root emergence requires tight regulation to ensure plant integrity and minimize the risk of pathogen infection. Using white lupin as a model representative for most plant species, we reveal a dual role for the phytohormone auxin during root primordium emergence in the control of cell wall modifications and overall cell wall chemical composition in a time and space regulated manner.

Introduction

Lateral root emergence is a highly regulated process that allows the newly formed lateral root primordium to progress through the outer layers of primary root tissues without major damages (Péret *et al.*, 2009). A central role for the hormone auxin as a regulator of emergence has been revealed using a combination of functional genomics (Swarup *et al.*, 2008, Kumpf *et al.*, 2013, Porco *et al.*, 2016,) and modeling (Péret *et al.*, 2013). These approaches have identified genetic components of the underlying regulatory network such as AUXIN RESPONSE FACTOR 7 (ARF7)/ARF19, LATERAL ORGAN BOUNDARIES-DOMAIN 29 (LBD29), INFLORESCENCE DEFICIENT IN ABSCISSION (IDA)/HAESA and the central role of the auxin transporters AUXIN TRANSPORTER-LIKE PROTEIN 3 (LAX3) and PIN-FORMED 3 (PIN3). Although *Arabidopsis thaliana* was demonstrated to be adequate for the identification and functional characterization of these genes, this plant model displays striking singularities in term of root anatomy and architecture. Indeed, each outer tissue is composed of only one layer of cells and unless using external stimuli such as high exogenous auxin levels or gravitational changes, the position of lateral roots cannot be accurately predicted. These specificities have hindered our ability to study cell wall responses during lateral root emergence and have called for the use of other plant models. We decided to focus on the production of structures called cluster roots that are found in various species belonging to 10 different botanical families and produced as an adaptation to low phosphate (Lamont, 2003). Cluster roots are secondary roots that produce numerous closely-spaced tertiary roots called rootlets, arranged in a cluster (Gallardo *et al.,* 2019) and as defined previously (Skene, 2001). Their location in the root system is highly predictable and due to the high number of new organs being produced, they allow for easy access without the need for external induction systems. White lupin (*Lupinus albus*) is a nitrogen-fixing annual plant from the Leguminosae family and is the only annual crop that can produce cluster roots. Building on the recent sequencing of its genome (Hufnagel *et al.*, 2020), pangenome (Hufnagel *et al.*, 2021) and the development of root transformation protocols (Sbabou *et al.*, 2010), it is now possible to use white lupin for molecular, functional and genetic studies. Rootlet morphogenesis in lupin differs from the simplified lateral root development of *Arabidopsis*. In contrast to

Arabidopsis, where the lateral root primordium is derived solely from mitotically activated pericycle cells, several tissue layers can contribute to the lupin rootlet primordium (Gallardo *et al.*, 2019), which is common in many angiosperms (Xiao *et al.*, 2019). Rootlet primordia cross these layers successfully without damaging the outer tissues despite their large number and proximity. Clusters of rootlets are produced regularly at a conserved distance on the first lateral roots emerging from the primary root, allowing easy and predictable access to large amounts of material, as needed for cell wall studies.

During the growth of the rootlet primordium, the surrounding cells are subjected to morphological adjustments including cell division and detachment. Yet, the plant cell wall is an obstacle to the latter, acting as a glue between cells. The cell wall is composed of polysaccharides including cellulose, hemicellulose and pectins together with structural proteins. This dynamic “frame-like” structure provides support and protection but is flexible enough to accommodate the cell fate. A recent report revealed the importance of pectin homogalacturonan methylesterification to regulate pre-branching site formation along the *Arabidopsis* primary root (Wachsman *et al.*, 2020). The authors also suggested that methylesterification in primordium-overlaying cell walls could play a role in facilitating their emergence. However, the modifications of cell wall chemistry and their consequences during lateral root emergence are still unclear.

Taking advantage of white lupin cluster roots and their synchronized rootlet emergence, we analyzed the transcriptomic responses to auxin and confirmed the predominant role of cell wall remodeling during this developmental process. Beyond the corroboration of the essential and conserved role of auxin as a major regulator of rootlet emergence in white lupin and across species, we focused our interest on an auxin-responsive polygalacturonase gene (*LaPG3*) expressed in the cell layer surrounding the rootlet primordium. Downregulation of *LaPG3* in transgenic lupin hairy roots delayed emergence, suggesting a major role for localized pectin degradation. In accordance, homogalacturonans were strongly demethylesterified in the emergence zone, making them susceptible to be targets of polygalacturonases. We further demonstrated that auxin treatment enhanced this effect. Yet, the methylesterification degree of

homogalacturonan did not vary specifically in cortical cells whether challenged by an emerging rootlet primordium or not. Intriguingly, rhamnogalacturonan-I (1,4)-β-D-galactans and extensin glycoproteins showed differential distribution, suggesting that they could be a hallmark of cell separation and/or mechanically challenged cells.

In this study, we propose a model where cluster root cortical cells prepare for the rootlet passage. An auxin signal triggers the demethylesterification of pectins along the cluster root, priming the cell wall for the sequential action of pectin degrading enzyme in primordia-overlaying cells.

Results

A conserved role for auxin during massive rootlet primordium emergence

Auxin is a central regulator in lateral root primordium initiation and emergence in higher plants (Du & Scheres, 2018). In white lupin, the natural auxin indole-3-acetic acid (IAA) induces the formation of cluster roots under phosphate deficiency (Neumann *et al.*, 2000; Meng *et al.*, 2013). To understand the precise contribution of auxin in the white lupin rootlet emergence process, we tested the effect of IAA on cluster root development. IAA exogenous application modified the root system architecture quite drastically (Fig. 1a, 1b and Supporting Information Fig. S1). Primary and secondary root elongation, including that of specialized cluster roots, was reduced by IAA treatment in a dose dependent manner with an unexpected decrease in rootlet number, while the overall rootlet density was unchanged (Fig. 1b). The short cluster root phenotype induced by IAA may lower the potential number of rootlet primordia initiated, thus likely explaining this counter intuitive effect of IAA. We assigned the rootlets as either emerged or to seven developmental stages of pre-emerged rootlet primordia, I-VII (Gallardo *et al.*, 2019). The analysis of rootlet stage distribution revealed that 70% were emerged at the highest concentration of IAA compared to only 30% in the control conditions (Fig. 1c). Accordingly, less primordia were found in stages I to VI in IAA treated plants compared to control plants. Overall, these data suggest that IAA modifies the lupin root architecture by promoting primordium emergence in a dose dependent fashion. To further understand how auxin influences lupin root architecture, we also

challenged the plants with naphthylphthalamic acid (NPA) (Abas *et al.*, 2021) and 1-naphthoxyacetic acid (1-NOA) (Laňková *et al.*, 2010), auxin efflux and influx inhibitors respectively (Fig. 1a and Supporting Information Fig. S1). NPA treatment strongly decreased rootlet number and density (Fig. 1b) and delayed rootlet primordium emergence (Fig. 1c). Inhibition of auxin influx machinery with 1-NOA had a mild negative effect on rootlet number but did not affect rootlet density (Fig. 1b). However, at 25 µM 1-NOA, emergence was delayed as shown by a higher number of primordia in the intermediate stages V-VI (Fig. 1c). Overall, these data demonstrate an important role of polar auxin transport in rootlet primordium morphogenesis and emergence. Auxin modulates the expression of a plethora of downstream target genes. To determine the extent of auxin transcriptional responses during rootlet emergence, the *DR5::nlsYFP* synthetic auxin reporter was expressed in lupin hairy roots. A strong activation of *DR5::nlsYFP* expression was found in the pericycle cell layer of cluster roots (Fig. 1d). We also detected a weak *DR5::nlsYFP* signal at the tip of the rootlet primordium starting from stage V. These results suggest that auxin transcriptional responses in secondary root primordia are conserved between lupin and *Arabidopsis*, although neighboring pericycle cells that are not necessarily engaged in the primordium developmental program might retain a high auxin response in white lupin.

Identification of gene clusters expressed in rootlets in response to auxin treatment

To better understand the effect of auxin on rootlet primordium emergence (Fig. 1c), we performed RNA sequencing on cluster root segments corresponding to the rootlet emergence zone (Fig. 2a). We collected samples treated with IAA at early (30 min, 1 and 2 hours) and late time points (6, 12, 24 and 48 hours) after treatment to assess the corresponding auxin-induced transcriptomic regulation. In total, 856 differentially expressed genes (DEG) compared to control treatment were detected and classified into seven clusters based on their expression patterns according to time point after treatment (Fig. 2b, Supporting Information Table S1). Three expression clusters contained most of the DEG, with 284 (cluster 1), 317 (cluster 2) and 141 (cluster 3) DEG, and these could be defined by distinct transcriptomic signatures (Fig. 2c). The

remaining DEG were grouped into four minor clusters showing oscillating response (cluster 4) or an early to intermediate upregulation in response to auxin (clusters 5, 6 and 7) (Supporting Information Fig. S2). We then conducted a gene ontology enrichment analysis to enable the functional interpretation of those clusters (Fig. 2c, Supporting Information Fig. S2 and Table S2). Cluster 1 included genes that were slightly upregulated by auxin in the early phase and then downregulated at the late time points. Genes in this cluster were mainly associated with oxidative stress-related processes with the identification of several putative peroxidase genes. Interestingly, ROS production and signaling have been recently proposed as positive regulators of lateral root emergence in *Arabidopsis* (Manzano *et al.*, 2014; Orman-Lizega *et al.*, 2016). Cluster 2 was assigned to the earliest auxin upregulated genes for which the expression peaked after 30 minutes of treatment and returned gradually to a low level after that (Fig. 2c). Those early-auxin induced genes were associated to processes such as defense responses and DNA-binding transcription factor activity. Cluster 3 differed by its expression and was defined by genes showing a late and steady auxin-induced upregulation starting after two hours of treatment (Fig. 2c). Remarkably, this cluster was enriched in genes with predicted roles in carbohydrate metabolic process, lyase and polygalacturonase activities. This suggests a prominent action of auxin on quick but transient transcriptional responses, rapid modulation of oxidative stress and most importantly a slow but durable cell wall remodeling mechanism occurring during rootlet emergence.

Defined expression of pectin remodeling genes is strongly associated with rootlet emergence

Cell wall properties of primordium-overlaying tissues greatly impact the emergence process. Previous studies discovered a large subset of cell wall remodeling genes involved in lateral root emergence in *Arabidopsis*. We established a list of orthologs for important known regulators of cell wall loosening during lateral root morphogenesis in *Arabidopsis* including the closest lupin orthologs of *EXPANSIN A1* (EXPA1 - *At1g69530*, Ramakrishna *et al.*, 2019), *EXPANSIN A17* (*EXPA17 - At4g01630*, Lee & Kim, 2013), *XYLOGLUCAN ENDOTRANSGLYCOSYLASE 6* (*XTR6*/*XTH23* -

At4g25810, Swarup *et al.*, 2008), homogalacturonan degrading enzymes *POLYGALACTURONASE LATERAL ROOT* (*PGLR - At5g14650*, Kumpf *et al.*, 2013) and *PECTIN LYASE A2* (*PLA2 - At1g67750*, Swarup *et al.*, 2008) and two homogalacturonan modifying enzymes *PECTIN METHYLESTERASE 3* and *PECTIN METHYLESTERASE INHIBITOR 9* (*PME3 - At3g14310* and *PMEI9 - At1g62770*, Hocq *et al.*, 2017a) (Supporting Information Fig. S3a). Next, we assessed the expression patterns of the selected candidates in lupin hairy roots transformed with promoter::GUS fusion constructs (Supporting Information Fig. S3b). Some of the selected candidate genes that were not identified in our transcriptomic dataset displayed overlapping gene expression patterns. *LaXTR1* and *LaPME1* were expressed in the cluster root tip and rootlet primordium, while expression of *LaEXP1* and *LaPMEI1* were restricted to the primordium base and pericycle cells (Supporting Information Fig. S3b). Interestingly, *proLaPMEI2::GUS* signal was found in the pericycle, endodermis and inner cortex surrounding rootlet primordia. To better understand the link between auxin and cell wall modification during rootlet emergence, we next analyzed the expression pattern of auxin-responsive genes present in cluster 3 (Supporting Information Fig. S4). The expression levels of these genes over the course of the auxin transcriptome (see Fig. 2) confirm that these genes enhance their expression over time after IAA treatment (Supporting Information Fig. S4). *O-GLYCOSYL HYDROLASE FAMILY 17L* (*LaOGH17L*) and *TRICHOME BIREFRINGENCE-LIKE 1* (*LaTBRL1*) were expressed in the elongation zone of the cluster root and at the base of the rootlet primordium (visible in stages VII-VIII). *PECTIN LYASE-LIKE 1* (*LaPLL1*) was expressed specifically in young vascular tissues (stages V – onward). *ProLaPLL2::GUS* displayed a broad signal in the meristematic zone of the cluster root and rootlet primordium. The galactose binding protein *DOMAIN OF UNKNOWN FUNCTION 642* gene (*LaDUF642*) was expressed in the elongation zone but also in the newly formed epidermis at the tip of the cluster root and rootlet primordium (stages V – onward) while *LaEXP2* expression was restricted to the epidermis in the elongation zone. *ProLaPG1::GUS* and *proLaPG2::GUS* activity were found in the vasculature including pericycle cells and *proLaPG2::GUS* was additionally found in the elongation zone of the emerging rootlet primordium (stages VII-VIII) (Supporting Information Fig. S4). We then used qPCR to

measure the expression of six selected cell wall related genes from cluster 3 in the cluster root “emergence zone” at T0, T24 and T48 after auxin treatment in comparison to the distal part of the cluster root, here after referred as the "CR tip zone” (Supporting Information Fig. S5). While *LaDUF642*, *LaOGH17L* and *LaTBRL1* show their highest expression in the CR tip zone at the early stage before auxin treatment (T0), the three putative pectin degrading enzymes *LaPLL1*, *LaPLL2* and *LaPG3* were preferentially expressed in the emergence zone 24 hours after the treatment.

Auxin-responsive *Lupinus albus POLYGALACTURONASE3* (*LaPG3*) is expressed in outer cortex cells overlaying rootlet primordium

Despite being expressed at a low basal level, *LaPG3* was highly responsive to auxin treatment and preferentially expressed in the rootlet emergence zone of the cluster root (Supporting Information Figs S5 and S6). The LaPG3 protein sequence presents a high percentage of identity (60%) when compared to its closest ortholog in *Arabidopsis*, POLYGALACTURONASE INVOLVED IN LATERAL ROOT (AtPGLR – AT5G14650) (Supporting Information Fig. S7a). Structural modeling of LaPG3 showed that it contains a common right-handed β-parallel fold characteristic for pectinases, including fungal endo-PGs and exo-PGs (Supporting Information Fig. S7b). Structural alignment with published PG structures (*Pectobacterium carotovorum*, *Aspergillus niger* and *Aspergillus aculeatus*) confirmed that LaPG3 is likely to act as an endo-PG, with conserved amino acid motifs at the active site including Asn211-Thr212-Asp213 (NTD), Asp234-Asp235 (DD), Gly256-His257-Gly258 (GHG) and Arg291-Ile292-Lys293 (RIK) (Supporting Information Fig. S7c, d). The activity of the LaPG3 promoter was undetectable in the cluster root elongation zone where there are no rootlet primordia (Supporting Information Fig. S8) but clearly visible in the meristematic zone and even more striking in primordium-overlaying cells, excluding the endodermis, starting from stages III-IV (Fig. 2d). *ProLaPG3::nlsYFP* transformed roots confirmed the expression of the fluorescent protein in cells that undergo separation (Supporting Information Fig. S9a). Interestingly, no signal was found in the mitotically activated endodermis and inner cortex cells. IAA treatment confirmed the responsiveness of *LaPG3* to the hormone, expanding the signal of *proLaPG3::GUS* to the external cortex (Fig. 2d).

These results suggest that spatial regulation of auxin-responsive *LaPG3* expression is important for rootlet primordium emergence. To understand the functional role of *LaPG3*, we expressed an artificial micro-RNA targeting its transcript under the control of the native promoter (*proLaPG3::amiR-LaPG3*) in lupin hairy roots (Supporting Information Fig. S9b). While cluster root length, rootlet number and density were not affected in hairy roots expressing *proLaPG3::amiR-LaPG3* compared to the control *proLaPG3::nlsYFP* (Supporting Information Fig. S9c), rootlet primordium emergence was significantly delayed in *proLaPG3::amiR-LaPG3* cluster roots (Fig. 2e). Gene expression analysis showed a 4-fold downregulation of *LaPG3* in *proLaPG3::amiR-LaPG3* cluster roots (Supporting Information Fig. S9d). Furthermore, the expression of the auxin-responsive *GRETCHEN-HAGEN3* (*GH3*) genes *LaGH3.3*, *LaGH3.5* and *LaGH3.6* were increased in *proLaPG3::amiR-LaPG3* cluster roots, possibly reflecting feedback between *LaPG3* and auxin homeostasis gene expression (Supporting Information Fig. S9d).

Oligogalacturonide profiling reveals auxin-induced pectin remodeling in cluster roots

Homogalacturonans (HG) are secreted into the cell wall as a polymer of galacturonic acid (GalA) which can be methylesterified and/or acetylated. It is suggested that the degree of methylesterification (DM) or acetylation (DA) of the HG plays a role in the availability of substrate for degradation enzymes such as polygalacturonases (Hocq *et al.*, 2017b). To understand the contribution of auxin-mediated changes in HG structure during rootlet emergence, we used an LC-MS/MS oligogalacturonide profiling method to reveal changes in HG composition in our cluster root samples (Voxeur *et al.*, 2019; Hocq *et al.*, 2020). For that purpose, we harvested segments corresponding to the "emergence zone" and the "CR tip zone" at T0, T24 hours and T48 hours after auxin treatment (Fig. 3a). We then used a microbial polygalacturonase from *Aspergillus aculeatus* to digest the cell wall fraction and performed oligogalacturonide fingerprinting as a way of analyzing the differences in homogalacturonan structure. Most of the oligogalacturonides released from the tip zone displayed a low degree of polymerization (DP ≤ 3) (Fig. 3b), which slightly accumulated over time in correlation with a decrease in

high DP oligogalacturonides (DP ≥ 4) (Fig. 3b). Principal component analysis revealed a strong effect of auxin treatment in the accumulation of low DP oligogalacturonides in the tip zone (GalA2 and GalA3) compared to mock conditions (Fig. 3b). Accordingly, oligogalacturonides of high DP (DP ≥ 4), although weakly represented, were reduced following auxin treatment (Fig. 3b). Those effects were visible after 24 hours of treatment and stable after 48 hours (Fig. 3b). In contrast, oligogalacturonides that were released from the emergence zone differed over the time course. For example, although GalA2 was weakly represented at T0 (< 1% of total oligogalacturonides) its proportion was significantly increased (reaching 10%) at T24 (Fig. 3c). In the meantime, high DP oligogalacturonides (DP ≥ 3) were less abundant in the total released fraction at T24 and T48 (Fig. 3c). However, auxin treatment had only a moderate impact on the DP of total oligogalacturonides released in the emergence zone and we observed a slight increase of GalA3 fraction while the GalA4 fraction was diminished (Fig. 3c). We next examined the DM and DA of the oligogalacturonides from the two segments of interest (Fig. 3d, e). In the cluster root tip zone, negligible changes in methylesterification or acetylation degrees occurred during the time course in control conditions, but auxin slightly induced a demethylesterification of GalA species at T24 (Fig. 3d). We observed a marginal auxin-induced increase of acetylated oligogalacturonides at T24, compensating a decrease seen in the control compared to T0 (Fig. 3d). Those effects were transient and stabilized at T48. This suggests a robust and early effect of auxin on HG modifications in the first 24 hours following the treatment in the CR tip zone. In the emergence zone, the already low level of released methylesterified oligogalacturonides was stable over time and was marginally reduced following auxin treatment after 24 hours (Fig. 3e). Remarkably, the proportion of acetylated oligogalacturonides declined during the control time course but was not affected by auxin (Fig. 3e) suggesting an important relation between early rootlet emergence events and acetylation of HG in control conditions. We briefly summarized our findings in the model shown in Fig. 3f. When the plants are grown in control conditions, the tip zone of the cluster root is not subjected to dramatic changes in term of pectin modifications such as HG methylesterification. A brief variation of acetylation status was observed after 24 hours but stayed stable over time. The DP of oligogalacturonides released was fairly high.

However, in the emergence zone in control conditions, we observed a low DM from the beginning of the time-course (T0), around 10 times less than in the tip zone. The DA was similar in both cluster root segments but decreased substantially after 24 hours in the emergence zone specifically. Oligogalacturonide DM was dramatically lower after auxin treatment in the tip zone and to a lesser degree in the emergence zone compared to the control conditions. Meanwhile, upon auxin treatment, oligogalacturonide DA remained stable in both zones while DP was reduced in the tip zone similarly to the untreated emergence zone.

Homogalacturonan demethylesterification is homogeneously triggered by auxin in the rootlet emergence zone

The spatial regulation of pectin remodeling enzyme activity is known to be essential for organ growth and development (Levesque-Tremblay *et al.*, 2015). In cluster roots, auxin caused demethylesterification of HG in the tip zone and to some degree in the emergence zone (Fig. 3d, e and f). To understand whether the observed changes might be tissue or cell specific, we assessed the pattern of pectin methylesterification in the emergence zone using a subset of monoclonal antibodies targeting HG of various DM status (Fig. 4). Immunolabeling of un-esterified HG with the LM19 antibody was uniform across rootlet primordium developmental stages and was not affected by auxin treatment (Fig. 4a). In contrast, JIM5, labeling HG stretches with a low DM, displayed a strongly increased signal in cortex cells when treated with auxin (Fig. 4b). The area directly touching the rootlet primordium was heavily marked, which could be explained by the high number of walls from collapsed cells in this particular location. We also noticed that phloem cells directly below the pericycle cell layer were labeled with JIM5, but this tended to decline in auxin-treated roots. These data suggest that auxin reduces the degree of HG methylesterification. However, pectins seemed to be preponderantly present in fully demethylesterified forms in this zone (Fig. 3e). When looking specifically at highly methylesterified HG using LM20, we observed that the cortex cell three-way junctions were strongly labeled (Fig. 4c). In contrast, weak to no labeling was found in other cell types in the epidermis and the stele. Auxin substantially decreased LM20 labeling homogeneously in all cortical cells. In agreement, JIM7, which recognizes a

highly methylesterified HG epitope, showed the same pattern as LM20 with a weaker signal in auxin-treated cluster roots (Fig. 4d). Overall, our results showed a clear positive effect of auxin in the removal of methylester groups from HG regardless of the location (overlaying a primordium or not) of the cortical cells.

(1,4)-β-D-galactan and extensins/type-I arabinogalactans are differentially distributed in primordium-overlaying cell walls

Rhamnogalacturonans-I (RG-I) are the second most abundant polymers in pectins and are composed of a rhamnose and galacturonic acid backbone with side chains of α-(1,5)-l-arabinans, (1,4)-β-D-galactans, and type-I arabinogalactans (Caffall & Mohnen 2009). Previous work have suggested that (1,4)-β-D-galactans might be involved in cell-cell adhesion depending on the developmental contexts (Moore *et al.*, 2014; Ng *et al.*, 2015). To determine whether (1,4)-β-D-galactans could play a role in rootlet emergence we examined their distribution using the specific LM5 antibody in cluster root cross sections (Fig. 5) (Andersen *et al.*, 2016). We noticed a significant reduction in the fluorescent signal for LM5 in the primordium-overlaying cortical cells from stage V onward in comparison to the early stages (stage I to IV) or the cortical cells facing the neighboring phloem poles. Interestingly, epidermis inner and shared cell walls were not labeled, indicating core cell wall differences between epidermis and cortex tissues. In contrast with HG methylesterification degree, RG-I (1,4)-β-D-galactan reduction was not altered by auxin treatment (Fig. 5). Contrary to the clear depletion of LM5 signal from stage IV onward in the control, we observed, at the same developmental stages, an increased distribution of a subset of antibodies targeting putative sugar epitopes from cell wall glycoproteins (Supporting Information Fig. S10). Extensin-specific JIM11 (Smallwood *et al.*, 1994) labeling was significatively increased in primordium-overlaying cortical cells in later stages (Supporting Information Fig. S10a). The same spatial distribution was observed for JIM93 and JIM94 antibodies, for which the epitope is suggested to be found in the arabinogalactan side chain of hydroxyproline-rich glycoproteins (HRGP) (Pattathil *et al.*, 2010; Hall *et al.*, 2013) (Supporting Information Fig. S10b, c). Labeling of JIM11, JIM93 and JIM94 were highly comparable in the stele, with an unusual labeling of the protoxylem, and in the walls separating the pericycle and

endodermis cell layers. These results suggest extensive RG-I remodeling in cortical-overlaying cells that are mechanically challenged by primordium outgrowth during its later developmental stages.

We summarized the main points of this study in a model describing the observed molecular events during rootlet emergence in white lupin cluster roots (Fig. 6). Auxin triggers demethylesterification of pectin as the root tissue differentiates (1), paving the way for LaPG3-mediated localized separation of the cortex cells during primordium growth (2). Radial heterogeneity of the cluster root is further supported by the observation of auxin-independent modifications of primordia overlaying cell walls such as the depletion of (1,4)-β-D-galactan and accumulation of extensins and type-I arabinogalactan epitopes (3).

Discussion

Since more than a century, botanists have been arguing about whether the secondary root emerges purely mechanically or is helped by the digestion of the outer cortical layers or both (Pond, 1908). Using white lupin, Pond elegantly compared the lateral root primordium to a boat cutting through the water, making its way out by pushing away the outer cortical tissues. His microscopic observations determined that separation but not digestion of the outer cortical cells occurs in the late stages, corresponding to what we now refer to as stage V onwards (Gallardo *et al.*, 2019). One century later, the central action of primordium tip-derived auxin in the activation of cell wall remodeling enzyme genes in the overlaying cells was described (Swarup *et al.*, 2008). However, to this date, the mechanistic modifications within the cell wall during lateral root emergence remain poorly described in most plant species. Here we showed the positive role of auxin treatment on rootlet emergence and found that the hormone strongly modulated cluster root transcriptomic responses (Fig. 1, Fig. 2b, c and Supporting Information Fig. S2, Table S2).

Cell wall related genes were steadily upregulated (Fig. 2c, cluster 3), including a polygalacturonase, *LaPG3*, specifically expressed in rootlet primordium overlaying cells (Fig. 2d, Supporting Information Fig. S9a). AmiRNA-driven down regulation of *LaPG3*

resulted in a modest delay of rootlet emergence in lupin hairy roots (Fig. 2e). Residual *LaPG3* transcripts or gene redundancy among this large gene family might explain this subtle phenotype. A simple explanation for this phenotype would be a reinforced cell wall and stronger cell adhesion in primordium-overlaying cells, slowing down the overall process of rootlet emergence. We also noticed the increased expression of auxin-responsive *GH3* genes in *proPG3::amiR-PG3* cluster roots (Supporting Information Fig. S9d). Auxin sensitivity is dampened in tobacco plants expressing fungal endo-PG and treatment with oligogalacturonide elicitors leads to the same effect in *Arabidopsis* (Ferrari *et al*., 2008; Savatin *et al*., 2011). Accordingly, we noticed a similar antagonism in the context of microRNA targeting *LaPG3* transcripts. Indeed, a low *LaPG3* expression could reduce oligogalacturonide-eliciting responses, thus alleviating the inhibition of auxin responses. This feedback loop between PG and auxin responses could help stabilize the rootlet emergence process by the inactivation of IAA via auxin-amido synthetase GH3.

Polygalacturonase activity requires structural modifications of the homogalacturonan pectic backbone and polygalacturonases are mostly active on demethylesterified stretches. Auxin plays an important role in the regulation of pectin methylesterase (PME) and PME inhibitor (PMEI) expression, which in turn modulates the degree of pectin methylesterification in diverse organs. However, auxin action on pectin methylesterification depends on the developmental process in question, positively regulating the removal of methylester groups in the shoot apical meristem while contrastingly promoting methylesterification during apical hook development (Braybrook & Peaucelle, 2013; Jonsson *et al*., 2021), for example. We were able to observe the dynamics of homogalacturonan methylesterification in the developing cluster root temporally, during early cluster root development, and spatially, discerning the most distal tip part (meristematic and elongation zone) and the rootlet emergence part (Fig. 3). A gradual demethylesterification of homogalacturonans occurred along the whole cluster root (Fig. 3d, e, Fig. 4) and was correlated with the release of oligogalacturonides of low degree of polymerization (Fig. 3b – e). This could be explained by the preferred affinity of *Aspergillus aculeatus* endo-PG2 for demethylesterified galacturonic acid stretches (Safran *et al*., 2021). As a result, highly

methylesterified pectin regions were most likely not released during our analysis. We hypothesize here that auxin causes changes in cell wall structure by regulating enzymes such as PME, allowing cell wall degradation in the emergence zone at specific locations marked by the expression of *LaPG3*. Such a tandem regulation of pectin degradation has been observed during pollen tetrad separation in *Arabidopsis*. *QUARTET1* (*QRT1*) encodes a PME that removes methylester groups, which stimulates *QUARTET3* (*QRT3*), a PG, to cleave homogalacturonans, allowing cell wall loosening (Rhee *et al.*, 2003; Francis *et al.*, 2006). *QRT1* is also specifically expressed at other locations of cell separation in *Arabidopsis*, including lateral root emergence-overlaying cells (Francis *et al.*, 2006).

The outer cortex is subject to enormous mechanical constraint in the rootlet emergence zone due to the growing primordium. Cell death can be observed in the endodermis and to a lesser extent in the cortex cells in species such as *Arabidopsis* (Escamez *et al.*, 2020). In white lupin, those layers (endodermis and inner cortex) divide and become included within the rootlet primordium. Microscopic observations of late-stage primordia (stage V onwards) indeed show collapsed outer cortex cells but whether cell death occurs remains to be proven (Gallardo *et al.*, 2019). Once the most difficult part of the rootlet's journey has been dealt with by the recruitment of endodermis and inner cortical cell divisions, one can assume that late emergence solely takes place due to the displacement of outer cortex and epidermis cells. The specific expression of *LaPG3* in those cells when a primordium grows underneath suggests, however, that degradation of the pectin-rich middle lamellae is crucial to reduce cell adhesion. Immunolabeling experiments with antibodies targeting homogalacturonan epitopes with diverse degrees of methylesterification confirmed that auxin triggered pectin demethylesterification in the emergence zone. However, we were not able to identify differential distribution of methylesterified and demethylesterified homogalacturonans in cortex cell walls challenged by a primordium or not (Fig. 4). Such a differential distribution of methylesterified pectins was recently reported at the junction between the lateral root primordium and endodermis in the early stages and later between endodermis and cortex in *Arabidopsis* (Wachsman *et al.*, 2020). By contrast, rhamnogalacturonan-I (RG-I) and glycoprotein epitopes did display this asymmetric distribution (Fig. 5, Supporting

Information Fig. S10). RG-I are thought to play a role in cell adhesion through crosslinks with cellulose microfibrils (Lin *et al.*, 2015). A loss of (1,4)-β-D-galactans has been correlated with fruit softening in the ripening process of apple and grapes (Moore *et al.*, 2014; Ng *et al.*, 2015). In this study, we detected a loss of (1,4)-β-D-galactan epitopes in the primordium-overlaying cortical cells, for which the effect was independent of auxin (Fig. 5).

Altogether, we propose a model for auxin-controlled cell separation during secondary root emergence. Auxin triggers homogalacturonan demethylesterification in the cluster root and induces the expression of a polygalacturonase at sites situated in front of growing primordia, resulting in cell wall remodeling allowing the emergence of numerous rootlets (Fig. 6). In most models of pectin structure, HG and RG-I are covalently linked (Zdunek *et al.*, 2020). The alteration of RG-I could increase the porosity of the cell wall, granting access to HG for degrading enzymes. Conversely, it is possible that the degradation of HG by polygalacturonases uncovers RG-I side chains allowing a modification of the galactan polymer. This impact on cell wall composition ensures that rootlet primordia push through the outer tissues without damaging them and most likely prevent the roots from pathogen attack at the base of the rootlets, offering a simple hypothesis to how so many rootlets can emerge almost synchronously for efficient soil exploration. The epidermis inner cell wall and the direct subepidermal cell layer were intriguingly not marked, reflecting different pectin composition and possibly mechanical properties of those cells. Nevertheless, it remains to be determined whether the (1,4)-β-D-galactan epitope loss in RG-I is part of a controlled active process of cell separation or is a passive consequence of cell wall remodeling. The tissue and cell specificity of cell wall modifications in white lupin cluster roots reflect the complexity of those mechanisms in one developmental context. Further studies will be needed to fully apprehend the role of cell wall remodeling across the phenomenal diversity of plant developmental processes.

Materials and Methods

Plant materials and growth conditions

White lupin (*Lupinus albus*) cv. AMIGA (from Florimond Desprez, France) used in this study was germinated in vermiculite and grown for three days under long day conditions (16 h light/8 h dark, 25 °C day/20 °C night, 65% relative humidity and PAR intensity 200 $\mu mol.m^2.s^{-1}$). The three-day-old seedlings were transferred to 1.6 L pots containing a phosphate-free hydroponic solution composed of the following: 400 µM $Ca(NO_3)$; 200 µM K_2SO_4; 54 µM $MgSO_4$; 0.24 µM $MnSO_4$; 0.1 µM $ZnSO_4$; 0.018 µM $CuSO_4$; 2.4 µM H_3BO_3; 0.03 µM Na_2MoO_4; 10 µM Fe-EDTA. Hydroponic medium was renewed weekly and constant oxygenation was provided by an air pump.

Chemical treatments and cluster root phenotyping

All chemicals used in this study were applied seven days after germination, at the onset of rootlet primordium development, directly in the hydroponic medium at the desired concentrations. The four uppermost cluster roots were sampled 48 hours after treatments and cleared in saturated aqueous chloral hydrate solution (250 g in 100 mL water) for two weeks before observation. Cluster root length (length of the parental lateral root), rootlet density and developmental stages of primordia were scored using a color camera on an Olympus BX61 epifluorescence microscope (Tokyo, Japan). For artificial microRNA cluster root characterization, we sampled individual cluster roots (each is an independent transformation event) of 4 to 6 hairy root composite plants one week after hydroponic transfer and screened them under the confocal microscope (Zeiss LSM780), searching for ubiquitous mCherry signal at 561 nm excitation. The binary vector used for hairy root phenotyping (pK7m24GW_CR) contains the verified internal control of transformation *proAtUBIQUITIN10/UBI::mCherry.* Hairy root experiments were conducted twice. Transformed cluster roots were transferred to chloral hydrate solution for phenotyping or frozen in liquid nitrogen for RNA extraction experiments. Transformed cluster roots showing obvious developmental irregularities such as root fusion or supernumerary xylem poles were excluded from the analysis.

GUS histochemical assay

Cluster roots (n > 10) were harvested from at least four transgenic plants for each construct and immediately fixed in ice-cold 90% acetone for 30 minutes, washed three times in 0.1 M phosphate buffer (pH 7) and incubated in X-Gluc buffer (0.1% X-Gluc;

50 mM phosphate buffer, pH 7, 2 mM potassium ferricyanide, 2 mM potassium ferrocyanide, 0.05% Triton X-100) for 1 to 24 hours depending on the construct. X-Gluc buffer was then removed and replaced by saturated aqueous chloral hydrate solution to allow clearing of the tissues.

Microscopic analysis

GUS-stained and *DR5::nlsYFP* and *LaPG3::nlsYFP* transformed cluster roots were embedded in 4% agarose (m/v) and cut with a vibratome to produce thick sections of 70 µm, (VT1000S, Leica Microsystems). The root sections were mounted on slides in 50% glycerol. Wild type (cv. AMIGA) cluster root thin sections of 6 µm were produced using a microtome (RM2165, Leica Microsystems). They were counterstained for 5 min either with 0.05% toluidine blue or with 0.1% ruthenium red in 1X phosphate buffer saline (1X PBS pH 7.4, Sigma Aldrich, P3813). GUS-stained and wild type cluster root sections were observed with a color camera on an Olympus BX61 epifluorescence microscope (Tokyo, Japan) with Camera ProgRes®C5 Jenoptik and controlled by ProgRes Capture software (Jenoptik, Jena, Germany). *DR5::nlsYFP* and *LaPG3::nlsYFP* transformed cluster roots were observed with a confocal microscope, including at least 10 transformed roots from a minimum of four hairy root composite plants (Zeiss LSM 780, details in “confocal microscopy” section below).

Immunolabeling experiments

Cross sections of 70 µm obtained with the vibratome were transferred onto chamber slides (Lab-teak, 177402) for immunostaining. They were first rinsed in 0.1 M glycine in 1X PBS and then twice in 1X PBS, each for 10 min. Sections were immersed in blocking buffer containing 5% bovine fetal serum (Sigma Aldrich, A9418) in 1X PBS at 4 °C overnight under gentle agitation. Monoclonal primary antibodies (list in Supplemental table 5) diluted 1/10 in the blocking buffer, were applied overnight at 4 °C under mild agitation. The sections were washed 3 times in 1X PBS for 10 min followed by two hours incubation in the secondary antibody (list in Supplemental table 5) diluted 1/500 in blocking buffer under gentle agitation. Sections were then washed three times in 1X PBS under mild agitation, 10 min each. The chambers were removed, and sections

mounted in 50% glycerol prior to observation. Immunolabeling experiments were repeated three times.

Confocal microscopy

Immunostained root sections were imaged on a confocal microscope (Zeiss LSM 780). Autofluorescence observation was performed using an argon laser at 405 nm and secondary antibodies were excited at 561 nm. Both were detected at a 566-679 nm window using the same settings (gain, offset and resolution which were manually set up) to allow quantification measurements (detailed in the Supplemental Methods S1). For *LaPG3::nlsYFP*, *DR5::nlsYFP* and screening of transformed cluster roots, mCherry internal control and nlsYFP were excited at 561 nm and 514 nm respectively and detected at 583-696 nm and 519-583 nm windows, respectively. Observations were made using Plan-Apochromat 10x/0.45 M27 and 20x/0.8 M27 objectives. Image acquisition was performed with the Zeiss ZEN black 2010 software and image analysis was conducted using the ZEN blue 2.3 lite software (Carl Zeiss Microscopy).

Oligogalacturonide characterization and quantification

OG characterization and quantification in cluster root samples from the emergence zone and tip zone were performed using the method published in Voxeur *et al.*, 2019.

Statistical analysis

Statistical analysis for phenotyping experiments and confocal image analysis were performed using GraphPad Prism version 9.0.2 for Windows (GraphPad Software, San Diego, California USA).

Details for gene expression analyses (RNA sequencing and qPCR experiments), phylogenetic trees, promoter::GUS and artificial microRNA cloning, hairy root transformation, homology modeling and fluorescence quantification are given in Supporting Information Methods S1.

Acknowledgments

We acknowledge Carine Alcon for technical support at the imaging facility MRI (Montpellier, France), a member of the national infrastructure France-BioImaging infrastructure supported by the French National Research Agency (ANR-10-INBS-04, «Investments for the future») and the microscopy facility at UPSC (Umeå, Sweden). We thank Serge Pilard (Analytical Platform, UPJV, France) for the LC-MS/MS analyses. We gratefully acknowledge Siamsa M. Doyle for critical reading of the manuscript. This work was supported by the Kempestiftelserna (Scholarship SMK 1759, F.J.), the Swedish Research Council Vetenskapsrådet grant VR-2020-03420 (F.J.), the Knut and Alice Wallenberg Foundation and Vinnova (Verket för Innovationssystem) (F.J., S.R.). This project has received funding from the European Research Council (ERC) under the European Union's Horizon 2020 research and innovation program (Starting Grant LUPINROOTS - grant agreement No 637420 to B.P.).

Author contributions

F.J. performed most of the experiments and analyzed results. A.S and F.J. analyzed RNAseq data, L.B. designed the binary vector pK7m24GW_CR for hairy root phenotyping experiments, C.C. and F.D. sampled and prepared RNA libraries for sequencing, F.J. and F.D performed and analyzed RT-qPCR experiments, J.S. generated *in silico* PG models, V.L. performed oligogalacturonide dosages, F.J., J.P. and V.L. analyzed OG dosages, F.J., S.R and B.P. designed the research, F.J, S.R and B.P. wrote the article. The authors declare no competing interest.

Data availability

White lupin gene identifiers and full genomic sequences are available on the White Lupin Genome Portal (Hufnagel *et al.*, 2020; www.whitelupin.fr). The RNAseq data have been deposited at NCBI under the temporary name "SUB9968787", bioproject "SAMN20089781".

References

Abas L, Kolb M, Stadlmann J, Janacek DP, Lukic K, Schwechheimer C, Sazanov LA, Mach L, Friml J, Hammes UZ. 2021. Naphthylphthalamic acid associates with and inhibits PIN auxin transporters. *Proceedings of the National Academy of Sciences* **118**.

Andersen MCF, Boos I, Marcus SE, Kračun SK, Rydahl MG, Willats WGT, Knox JP, Clausen MH. 2016. Characterization of the LM5 pectic galactan epitope with synthetic analogues of β-1,4-d-galactotetraose. *Carbohydrate Research* **436**: 36–40.

Braybrook SA, Peaucelle A. 2013. Mechano-Chemical Aspects of Organ Formation in Arabidopsis thaliana: The Relationship between Auxin and Pectin. *PLOS ONE* **8**: e57813.

Caffall KH, Mohnen D. 2009. The structure, function, and biosynthesis of plant cell wall pectic polysaccharides. *Carbohydrate Research* **344**: 1879–1900.

Du Y, Scheres B. 2018. Lateral root formation and the multiple roles of auxin. *Journal of Experimental Botany* **69**: 155–167.

Escamez S, André D, Sztojka B, Bollhöner B, Hall H, Berthet B, Voß U, Lers A, Maizel A, Andersson M, *et al.* 2020. Cell Death in Cells Overlying Lateral Root Primordia Facilitates Organ Growth in Arabidopsis. *Current Biology* **30**: 455-464.e7.

Ferrari S, Galletti R, Pontiggia D, Manfredini C, Lionetti V, Bellincampi D, Cervone F, De Lorenzo G. 2008. Transgenic Expression of a Fungal endo-Polygalacturonase Increases Plant Resistance to Pathogens and Reduces Auxin Sensitivity. *Plant Physiology* **146**: 669–681.

Francis KE, Lam SY, Copenhaver GP. 2006. Separation of Arabidopsis Pollen Tetrads Is Regulated by QUARTET1, a Pectin Methylesterase Gene. *Plant Physiology* **142**: 1004–1013.

Gallardo C, Hufnagel B, Casset C, Alcon C, Garcia F, Divol F, Marquès L, Doumas P, Péret B. 2019. Anatomical and hormonal description of rootlet primordium development along white lupin cluster root. *Physiologia Plantarum* **165**: 4–16.

Hall HC, Cheung J, Ellis BE. **2013**. Immunoprofiling reveals unique cell-specific patterns of wall epitopes in the expanding Arabidopsis stem. *The Plant Journal* **74**: 134–147.

Hocq L, Guinand S, Habrylo O, Voxeur A, Tabi W, Safran J, Fournet F, Domon J-M, Mollet J-C, Pilard S, *et al.* 2020. The exogenous application of AtPGLR, an endo-polygalacturonase, triggers pollen tube burst and repair. *The Plant Journal* **103**: 617–633.

Hocq L, Pelloux J, Lefebvre V. **2017a**. Connecting Homogalacturonan-Type Pectin Remodeling to Acid Growth. *Trends in Plant Science* **22**: 20–29.

Hocq L, Sénéchal F, Lefebvre V, Lehner A, Domon J-M, Mollet J-C, Dehors J, Pageau K, Marcelo P, Guérineau F, *et al.* 2017b. Combined Experimental and Computational Approaches Reveal Distinct pH Dependence of Pectin Methylesterase Inhibitors1. *Plant Physiology* **173**: 1075–1093.

Hufnagel B, Marques A, Soriano A, Marquès L, Divol F, Doumas P, Sallet E, Mancinotti D, Carrere S, Marande W, *et al.* 2020. High-quality genome sequence of white lupin provides insight into soil exploration and seed quality. *Nature Communications* **11**: 492.

Hufnagel B, Soriano A, Taylor J, Divol F, Kroc M, Sanders H, Yeheyis L, Nelson M, Péret B. **2021**. Pangenome of white lupin provides insights into the diversity of the species. *Plant Biotechnology Journal* **n/a**.

Jonsson K, Lathe RS, Kierzkowski D, Routier-Kierzkowska A-L, Hamant O, Bhalerao RP. **2021**. Mechanochemical feedback mediates tissue bending required for seedling emergence. *Current Biology* **31**: 1154-1164.e3.

Kumpf RP, Shi C-L, Larrieu A, Stø IM, Butenko MA, Péret B, Riiser ES, Bennett MJ, Aalen RB. **2013**. Floral organ abscission peptide IDA and its HAE/HSL2 receptors control cell separation during lateral root emergence. *Proceedings of the National Academy of Sciences* **110**: 5235–5240.

Lamont BB. **2003**. Structure, ecology and physiology of root clusters – a review. *Plant and Soil* **248**: 1–19.

Laňková M, Smith RS, Pešek B, Kubeš M, Zažímalová E, Petrášek J, Hoyerová K. **2010**. Auxin influx inhibitors 1-NOA, 2-NOA, and CHPAA interfere with membrane dynamics in tobacco cells. *Journal of Experimental Botany* **61**: 3589–3598.

Lee HW, Kim J. **2013**. EXPANSINA17 Up-Regulated by LBD18/ASL20 Promotes Lateral Root Formation During the Auxin Response. *Plant and Cell Physiology* **54**: 1600–1611.

Levesque-Tremblay G, Pelloux J, Braybrook SA, Müller K. **2015**. Tuning of pectin methylesterification: consequences for cell wall biomechanics and development. *Planta* **242**: 791–811.

Lin D, Lopez-Sanchez P, Gidley MJ. **2015**. Binding of arabinan or galactan during cellulose synthesis is extensive and reversible. *Carbohydrate Polymers* **126**: 108–121.

Manzano C, Pallero-Baena M, Casimiro I, De Rybel B, Orman-Ligeza B, Van Isterdael G, Beeckman T, Draye X, Casero P, del Pozo JC. **2014**. The Emerging Role of Reactive Oxygen Species Signaling during Lateral Root Development. *Plant Physiology* **165**: 1105–1119.

Meng ZB, You XD, Suo D, Chen YL, Tang C, Yang JL, Zheng SJ. **2013**. Root-derived auxin contributes to the phosphorus-deficiency-induced cluster-root formation in white lupin (Lupinus albus). *Physiologia Plantarum* **148**: 481–489.

Moore JP, Fangel JU, Willats WGT, Vivier MA. **2014**. Pectic-β(1,4)-galactan, extensin and arabinogalactan–protein epitopes differentiate ripening stages in wine and table grape cell walls. *Annals of Botany* **114**: 1279–1294.

Neumann G, Massonneau A, Langlade N, Dinkelaker B, Hengeler C, Römheld V, Martinoia E. **2000**. Physiological Aspects of Cluster Root Function and Development in Phosphorus-deficient White Lupin (Lupinus albus L.). *Annals of Botany* **85**: 909–919.

Ng JKT, Schröder R, Brummell DA, Sutherland PW, Hallett IC, Smith BG, Melton LD, Johnston JW. **2015**. Lower cell wall pectin solubilisation and galactose loss during

early fruit development in apple (Malus x domestica) cultivar 'Scifresh' are associated with slower softening rate. *Journal of Plant Physiology* **176**: 129–137.

Orman-Ligeza B, Parizot B, de Rycke R, Fernandez A, Himschoot E, Van Breusegem F, Bennett MJ, Périlleux C, Beeckman T, Draye X. **2016**. RBOH-mediated ROS production facilitates lateral root emergence in Arabidopsis. *Development (Cambridge, England)* **143**: 3328–3339.

Pattathil S, Avci U, Baldwin D, Swennes AG, McGill JA, Popper Z, Bootten T, Albert A, Davis RH, Chennareddy C, *et al.* 2010. A Comprehensive Toolkit of Plant Cell Wall Glycan-Directed Monoclonal Antibodies. *Plant Physiology* **153**: 514–525.

Péret B, De Rybel B, Casimiro I, Benková E, Swarup R, Laplaze L, Beeckman T, Bennett MJ. **2009**. Arabidopsis lateral root development: an emerging story. *Trends in Plant Science* **14**: 399–408.

Péret B, Middleton AM, French AP, Larrieu A, Bishopp A, Njo M, Wells DM, Porco S, Mellor N, Band LR, *et al.* 2013. Sequential induction of auxin efflux and influx carriers regulates lateral root emergence. *Molecular Systems Biology* **9**: 699.

Pond RH. **1908**. Emergence of Lateral Roots. *Botanical Gazette* **46**: 410–421.

Porco S, Larrieu A, Du Y, Gaudinier A, Goh T, Swarup K, Swarup R, Kuempers B, Bishopp A, Lavenus J, *et al.* 2016. Lateral root emergence in Arabidopsis is dependent on transcription factor LBD29 regulating auxin influx carrier LAX3. *Development* **143**: 3340–3349.

Ramakrishna P, Ruiz Duarte P, Rance GA, Schubert M, Vordermaier V, Vu LD, Murphy E, Vilches Barro A, Swarup K, Moirangthem K, *et al.* 2019. EXPANSIN A1-mediated radial swelling of pericycle cells positions anticlinal cell divisions during lateral root initiation. *Proceedings of the National Academy of Sciences* **116**: 8597–8602.

Rhee SY, Osborne E, Poindexter PD, Somerville CR. **2003**. Microspore Separation in the quartet 3 Mutants of Arabidopsis Is Impaired by a Defect in a Developmentally Regulated Polygalacturonase Required for Pollen Mother Cell Wall Degradation. *Plant Physiology* **133**: 1170–1180.

Safran J, Habrylo O, Cherkaoui M, Lecomte S, Voxeur A, Pilard S, Bassard S, Pau-Roblot C, Mercadante D, Pelloux J, *et al.* 2021. New insights into the specificity and processivity of two novel pectinases from Verticillium dahliae. *International Journal of Biological Macromolecules* **176**: 165–176.

Savatin DV, Ferrari S, Sicilia F, De Lorenzo G. **2011**. Oligogalacturonide-Auxin Antagonism Does Not Require Posttranscriptional Gene Silencing or Stabilization of Auxin Response Repressors in Arabidopsis1[W]. *Plant Physiology* **157**: 1163–1174.

Sbabou L, Bucciarelli B, Miller S, Liu J, Berhada F, Filali-Maltouf A, Allan D, Vance C. **2010**. Molecular analysis of SCARECROW genes expressed in white lupin cluster roots. *Journal of Experimental Botany* **61**: 1351–1363.

Skene KR. 2001. **Cluster roots: model experimental tools for key biological problems**. *Journal of Experimental Botany* **52**: 479-485.

Smallwood M, Beven A, Donovan N, Neill SJ, Peart J, Roberts K, Knox JP. **1994**. Localization of cell wall proteins in relation to the developmental anatomy of the carrot root apex. *The Plant Journal* **5**: 237–246.

Swarup K, Benková E, Swarup R, Casimiro I, Péret B, Yang Y, Parry G, Nielsen E, De Smet I, Vanneste S, *et al.* 2008. The auxin influx carrier LAX3 promotes lateral root emergence. *Nature Cell Biology* **10**: 946–954.

Voxeur A, Habrylo O, Guénin S, Miart F, Soulié M-C, Rihouey C, Pau-Roblot C, Domon J-M, Gutierrez L, Pelloux J, *et al.* 2019. Oligogalacturonide production upon Arabidopsis thaliana–Botrytis cinerea interaction. *Proceedings of the National Academy of Sciences* **116**: 19743–19752.

Wachsman G, Zhang J, Moreno-Risueno MA, Anderson CT, Benfey PN. **2020**. Cell wall remodeling and vesicle trafficking mediate the root clock in Arabidopsis. *Science* **370**: 819–823.

Xiao TT, van Velzen R, Kulikova O, Franken C, Bisseling T. **2019**. Lateral root formation involving cell division in both pericycle, cortex and endodermis is a common and ancestral trait in seed plants. *Development* **146**.

Zdunek A, Pieczywek PM, Cybulska J. **2021**. The primary, secondary, and structures of higher levels of pectin polysaccharides. *Comprehensive Reviews in Food Science and Food Safety* **20**: 1101–1117.

Figures

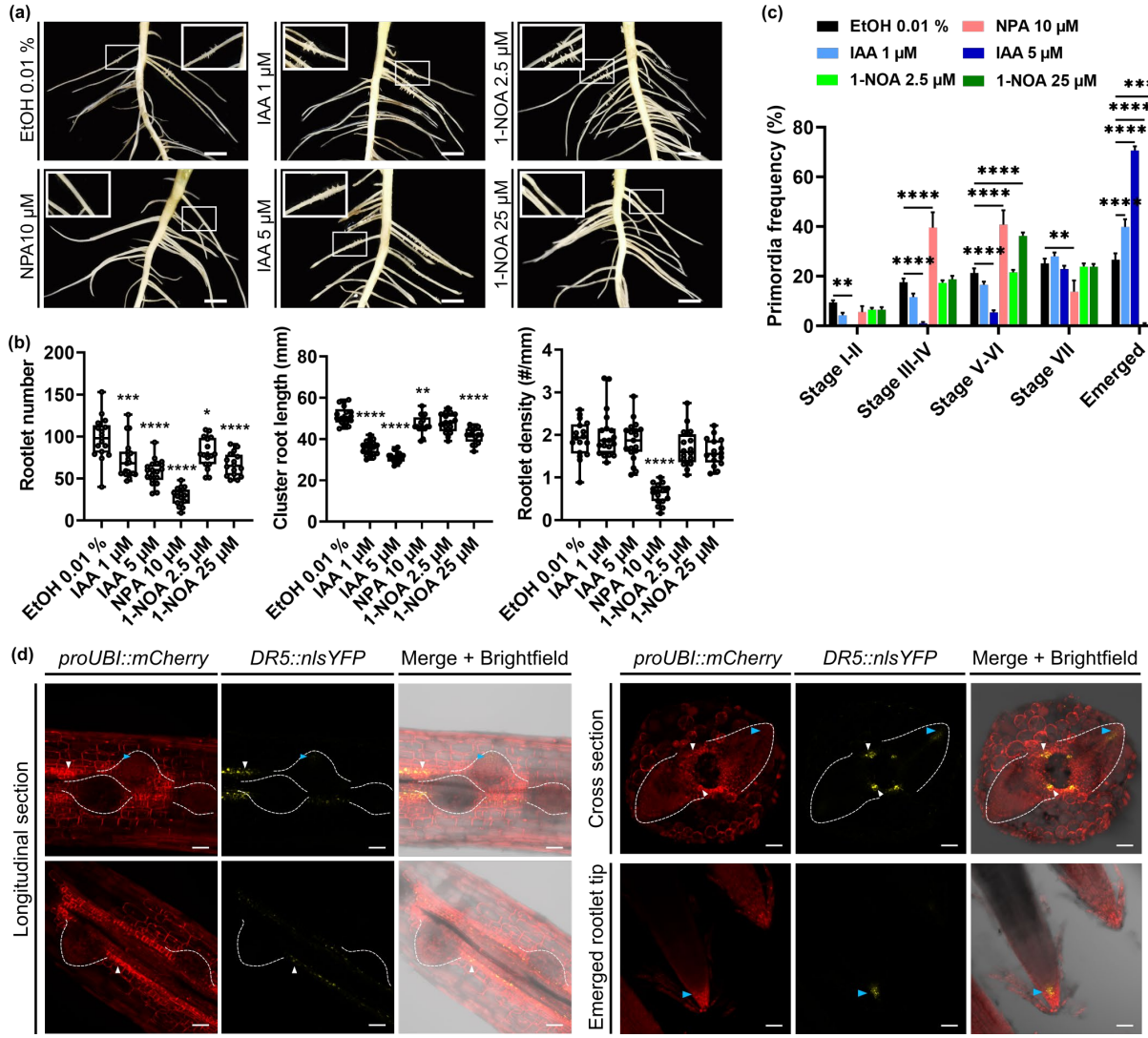

Figure 1. Auxin regulates rootlet development and primordium emergence.

(a) Representative pictures of the cluster roots from nine-day-old *L. albus* grown in hydroponics medium after two days supplemented with 0.01% ethanol (EtOH; control treatment), 10 µM NPA, 1 µM IAA, 5 µM IAA, 2.5 µM 1-NOA or 25 µM 1-NOA. A close up of the rootlet emergence zone is displayed for each picture. Scale bars: 1 cm. **(b)** Rootlet number, cluster root length and rootlet density in the 4 uppermost cluster roots in plants treated with 0.01% ethanol (n = 17), 10 µM NPA (n = 16), 1 µM IAA (n = 19), 5 µM IAA (n = 19), 2.5 µM 1-NOA (n = 16) or 25 µM 1-NOA (n = 16). Rootlet number and density includes both emerged rootlets and pre-emerged primordia. Data are

represented as mean ± SEM. Statistical significance (compared to control) was computed by the Dunnett multiple comparison test: ****: pVal < 0.001, ***: pVal < 0.005, **: pVal < 0.01, *: pVal < 0.05. **(c)** Frequency of primordium stages found in the 4 uppermost cluster roots in plants treated with 0.01% ethanol (black bars, n = 17), 10 µM NPA (pink bars, n = 16), 1 µM IAA (light blue bars, n = 19), 5 µM IAA (dark blue bars, n = 19), 2.5 µM 1-NOA (light green bars, n = 16) or 25 µM 1-NOA (dark green bars, n = 16). Data are represented as mean ± SEM. Statistical significance (compared to control) was computed by the Dunnett multiple comparison test: ****: pVal < 0.001, ***: pVal < 0.005, **: pVal < 0.01, *: pVal < 0.05. **(d)** Synthetic auxin response reporter DR5 is active in the pericycle cell layer of the rootlet emergence zone and at the tips of rootlet primordia. *ProUBI::mCherry* is an internal positive control of transformation. Free-hand sections were done immediately after harvesting fresh transformed roots. White dashed lines outline rootlet primordia, white and blue arrows respectively indicate pericycle cell layer and the tip of a primordium/rootlet. Scale bars: 100 µm.

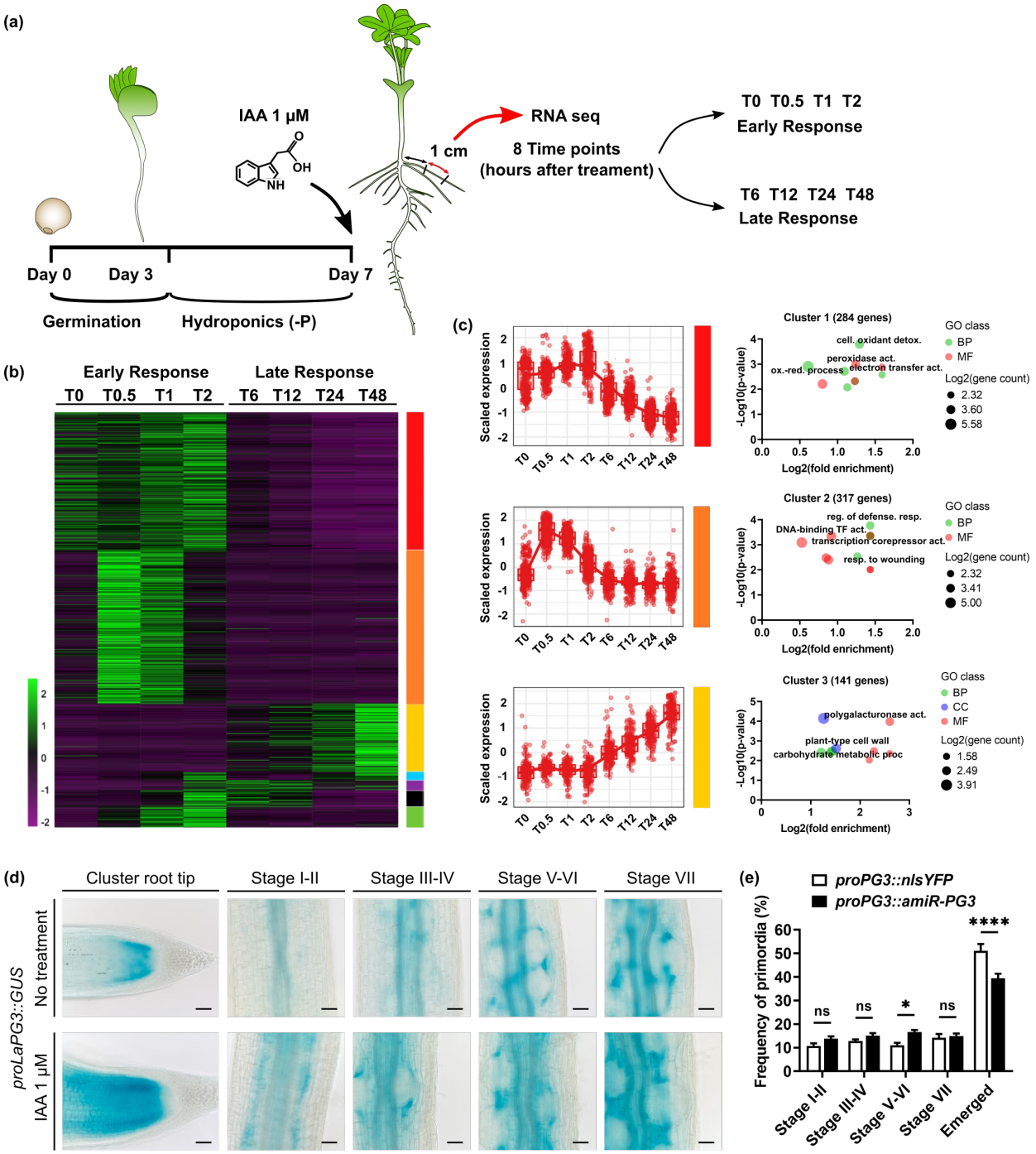

Figure 2. Auxin transcriptome landscape identifies cell wall related genes linked to rootlet emergence.

(a) Auxin RNA sequencing experiment overview. Lupin seeds were germinated in vermiculite for three days before the seedlings ("mohawk" stage) were transferred to hydroponic medium without phosphate (-P) to induce the formation of cluster roots (Day

3). Four days later (Day 7), 1 µM IAA was added to the hydroponic medium and 1 cm segments of cluster roots 1 cm distant from the primary root, corresponding to the emergence zone, were harvested for RNA extraction and further RNA sequencing at 8 different time points: T0 (just before the treatment), half an hour (T0.5), one hour (T1) and two hours (T2) after the treatment to assess the early auxin transcriptomic responses and six hours (T6), 12 hours (T12), one day (T24) and two days (T48) later for the late auxin transcriptomic responses. **(b)** Heatmap of white lupin auxin-regulated transcripts. Normalized expression levels are shown as a z-score (See Material and Methods section for further details) and hierarchical clusters of the differentially expressed genes (DEG) are displayed by the colored squares on the right of the heatmap. Expression patterns for each cluster are shown in Supporting Information Figure S2. **(c)** The three largest expression clusters (red, orange and yellow) show distinct gene expression patterns and are enriched in specific gene ontology terms. GO terms of significant importance are shown (red circle: molecular function, MF; green circle: biological process, BP; blue circle: cellular component, CC). **(d)** *proLaPG3::GUS* localization in cluster root tips and at different rootlet primordium development stages in regular hydroponic medium (top) and after 48 hours of 1 µM IAA treatment (bottom). Scale bars: 100 µm. **(e)** Frequency of primordium stages in cluster roots from hairy root composite plants expressing *proPG3::amiR-PG3* (n = 27 roots) and *proPG3::nlsYFP* (n = 28) as a control. Data are represented as mean ± SEM. Statistical significance was computed by the Šídák's multiple comparisons test. *: pVal < 0.05, ****: pVal < 0.001, ns: non-significant.

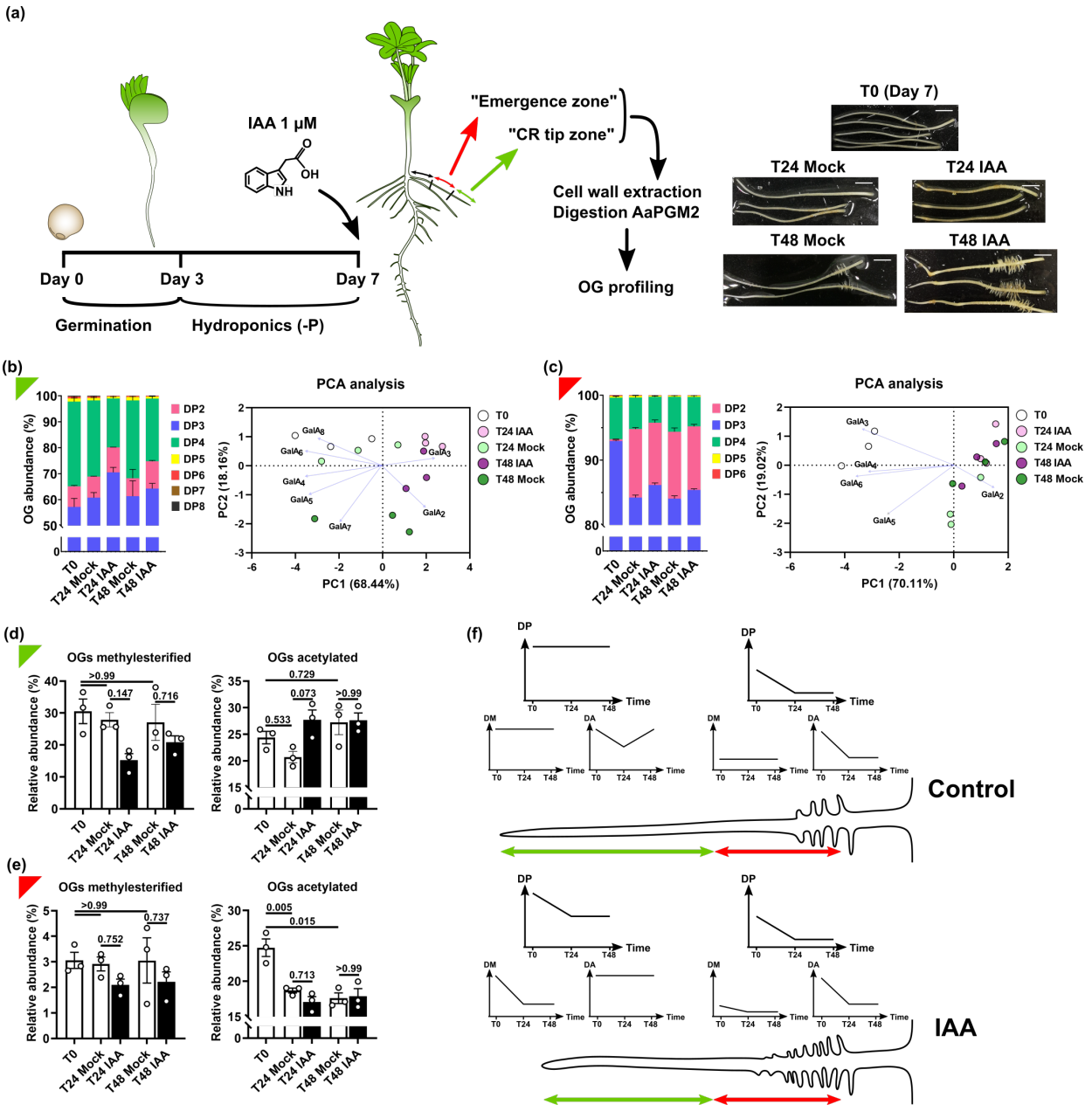

Figure 3. Oligogalacturonide profiling reveals auxin-induced pectin remodeling in cluster roots.

(a) Auxin oligogalacturonide (OG) profiling experiment overview. Lupin seeds germinated in vermiculite for three days before the seedlings ("mohawk" stage) were transferred to hydroponic medium without phosphate (-P) to induce the formation of cluster roots (Day 3). Four days later (Day 7), 1 µM IAA or 0.01% ethanol (Mock) were added to the hydroponic medium and 1 cm segments of cluster roots 1 cm distant from

the primary root (hereafter named emergence zone, red color code) and the distal part of the cluster root (CR tip zone, green color code) were harvested for cell wall extraction, digestion with *Aspergillus aculeatus* endo-polygalacturonase M2 (AaPGM2) and OG profiling according to Voxeur *et al.*, 2019. The samples shown in the pictures (bars: 0.5 mm) were dissected and collected at T0 (just before the auxin treatments), and at one day (T24) and two days (T48) after auxin treatments. **(b)** Effect of the auxin treatment on GalAx species released in the "CR tip zone" during the time course previously described. Left plot: OG abundance (% of total OG detected) in the CR tip zone at T0 and 24 and 48 hours after treatment with ethanol (T24 and T48 Mock) or IAA (T24 and T48 IAA). Right plot: bi-dimensional plot of principal components calculated by performing PCA of the different OG species relative abundances (grouped by degree of polymerization) for each treatment and time point (3 replicates each). Vectors describe the contribution of the OG species to the biplot. **(c)** Effect of the auxin treatment on GalAx species released in the "emergence zone" during the time course previously described. See **b** for descriptions of the plots. Full statistics for **b** and **c** are available in the Supplemental Table S3. **(d)** Relative abundance of methylesterified OG (GalAxMemAcn, x, m ≥ 1, n ≥ 0) or acetylated OG (GalAxMemAcn, x, m ≥ 0, n ≥ 1) from the CR tip zone. Statistical significance was computed using Tukey's multiple comparison test, adjusted p value numbers are reported. Data are represented as mean ± SEM. **(e)** Relative abundance of methylesterified OG (GalAxMemAcn, x, m ≥ 1, n ≥ 0) or acetylated OG (GalAxMemAcn, x, m ≥ 0, n ≥ 1) from the emergence zone. Statistical significance was computed using Tukey's multiple comparison test, adjusted p value numbers are reported. Data are represented as mean ± SEM. **(f)** Schematic representation of OG profiling experiment results. Top: control condition. Bottom: IAA-treated condition. Green and red arrows represent the CR tip and emergence zones, respectively. Plots representing the DP, DM and DA status of oligogalacturonides during the time course are displayed above each relevant zone. DP, degree of polymerization; DM, degree of methylesterification; DA, degree of acetylation.

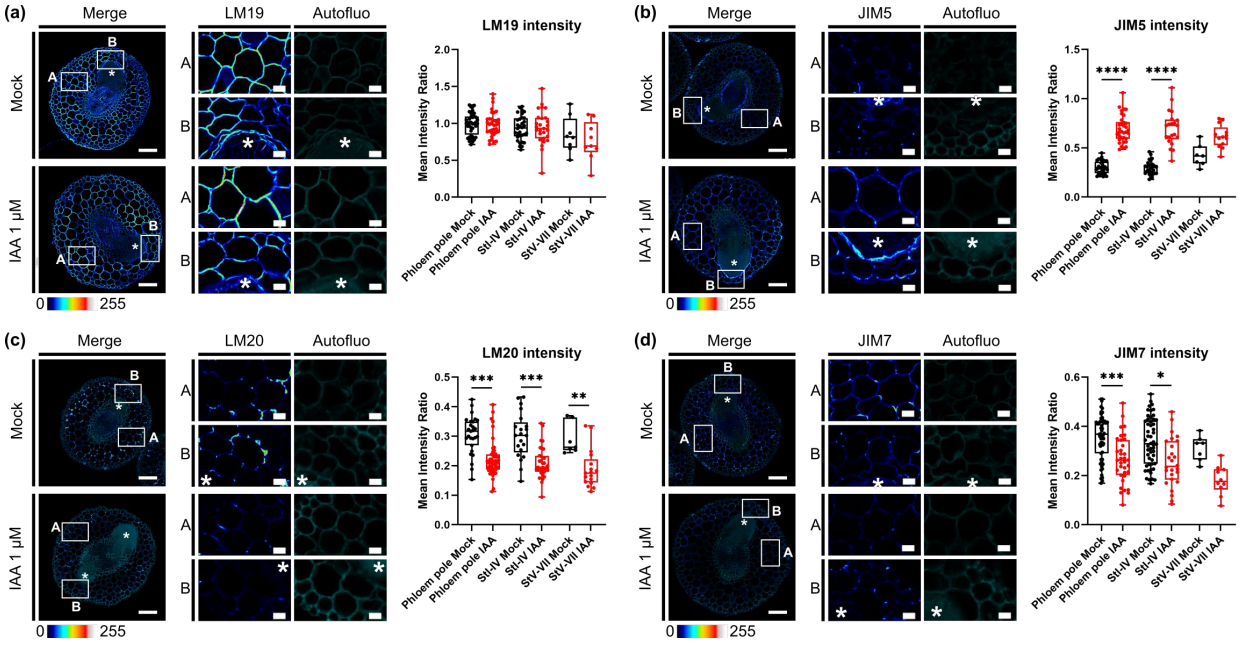

Figure 4. Auxin induces HG demethylesterification in cluster root cortical tissues independently of rootlet primordium emergence stage and location.

Immunolabeling with homogalacturonan (HG) specific LM19 (unesterified HG) **(a)**, JIM5 (low methylesterified HG) **(b)**, LM20 **(c)** and JIM7 (highly methylesterified HG) **(d)** antibodies in cluster root cross sections 2 days after treatment with 1 µM IAA or Mock (Ethanol 0.01%). Scale bar for the whole cross sections: 100 µm, scale bar for the close-ups: 20 µm. Boxplot represents antibody intensity defined as the ratio of secondary antibody signal to autofluorescence signal (Autofluo) in the "mechanically unchallenged" cortical tissues (Close-up "A"; phloem pole) or overlaying early (stage I to IV) and late (Close-up "B"; stage V to VII) rootlet primordia. Asterisks indicate the rootlet primordium localization on the micrograph. False color code depicts relative secondary antibody fluorescent intensity. All data points are displayed, whiskers show minimal and maximal values (**a**, mock: phloem pole: n = 40 sections, Stl-IV: n = 32, StV-VII: n = 8; IAA: phloem pole: n = 34, Stl-IV: n = 27, StV-VII: n = 9; **b**, mock: phloem pole: n = 36, Stl-IV: n = 29, StV-VII: n = 7; IAA: phloem pole: n = 34, Stl-IV: n = 21, StV-VII: n = 13; **c**, mock: phloem pole: n = 27, Stl-IV: n = 21, StV-VII: n = 7; IAA: phloem pole: n = 46, Stl-IV: n = 33, StV-VII: n = 17; **d**, mock: phloem pole: n = 59, Stl-IV: n = 52, StV-VII: n = 7; IAA: phloem pole: n = 35, Stl-IV: n = 26, StV-VII: n = 10). Statistical significance was

computed with the Kruskal-Wallis test. ****: pVal < 0.001, ***: pVal < 0.005, **: pVal < 0.01, *: pVal < 0.05.

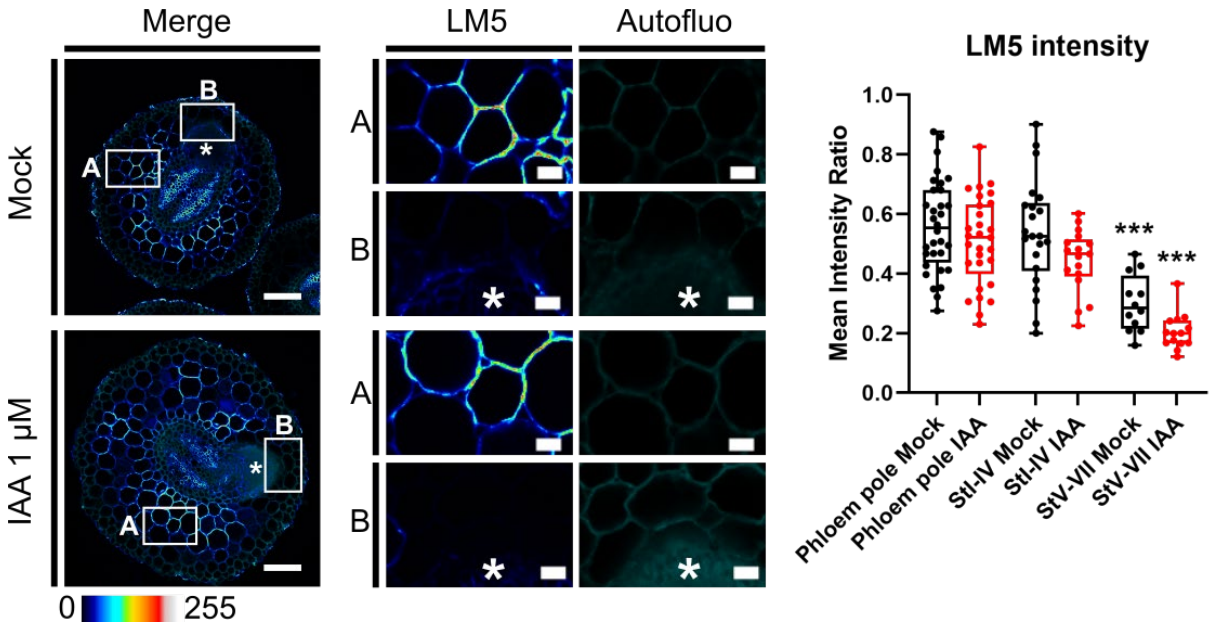

Figure 5. Rhamnogalacturonan I (1,4)-β-D-galactan is depleted in rootlet primordium-overlaying cells independently of auxin treatment.

Immunohistochemistry with (1,4)-β-D-galactan specific LM5 antibody in cluster root cross sections 2 days after treatment with 1 µM IAA or Mock (Ethanol 0.01%). Scale bar for the whole cross sections: 100 µm, scale bar for the close-ups: 20 µm. Asterisks indicate the rootlet primordium localization on the micrograph. False color code depicts relative secondary antibody fluorescent intensity. Boxplot represents the antibody intensity defined as the ratio of secondary antibody (Alexa 546) signal to autofluorescence signal in the "mechanically unchallenged" cortical tissues (Close-up "A"; phloem pole) or those overlaying early (stage I to IV) and late (Close-up "B"; stage V to VII) rootlet primordia. All data points are displayed, whiskers show minimal and maximal values (mock: phloem pole: n = 32 sections, StI-IV: n = 22, StV-VII: n = 12; IAA: phloem pole: n = 29, StI-IV: n = 17, StV-VII: n = 14). Statistical significance (compared to "phloem pole" mean intensity ratio mock conditions) was computed with the Kruskal-Wallis test. ***: pVal < 0.005.

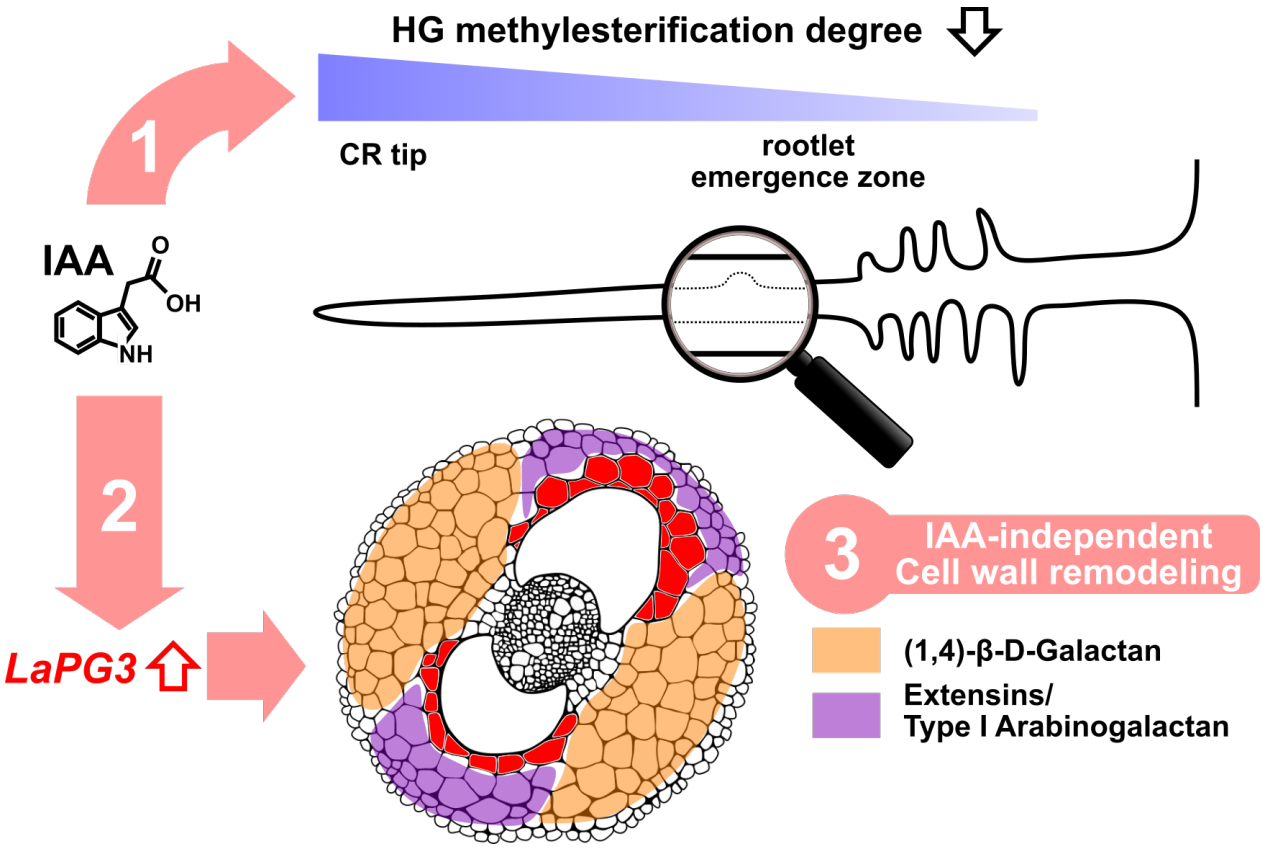

Figure 6. Model of cell wall regulations occurring in white lupin cluster root during rootlet primordium emergence.

During cluster root development, IAA induces the expression of a plethora of cell wall remodeling genes resulting in a decrease in homogalacturonan (HG) methylesterification degree along the cluster root (1). In the meantime, IAA strongly induces the expression of *LaPG3* in the rootlet primordium overlaying cortical cells, promoting its emergence (colored in red) (2). Independently of auxin action, we observed a depletion in (1,4)-β-D-Galactan (colored in orange) and a concomitant accumulation of Extensins/Type I Arabinogalactan epitopes in the primordium overlaying cortical cells (colored in purple) (3).